Wirelessly Powered Implantable System for Wireless Long-Term Monitoring of Intracranial Pressure

M. Waqas A. Khan, Lauri Sydänheimo, Toni Björninen, Leena Ukkonen

Department of Electronics and Communications Engineering, Tampere University of Technology, Tampere, Finland

Email: {muhammad.khan, lauri.sydanheimo, toni.bjorninen, leena.ukkonen}@tut.fi

Abstract—**This paper presents the pressure readout results from a piezoresistive pressure sensor in a biological environment mimicking the human head properties for intracranial pressure (ICP) monitoring application. The piezoresistive pressure sensor is powered wirelessly through inductively coupled antennas. After successful activation of the sensor, the pressure readout is demonstrated from 0 mmHg to 30 mmHg with a resolution of one mmHg.**

Keywords— Wireless inductive powering, intracranial pressure, piezoresistive pressure sensor and inductive coupling.

I. INTRODUCTION

Cranial cavity can be considered a fixed space with three main components: blood, cerebrospinal fluid (CSF) and brain and they are in volume equilibrium. The brain parenchyma is nearly incompressible, but physiological autoregulation mechanism controls the volume of the other two to maintain constant intracranial pressure (ICP) [1]. If the compensatory reserves are exhausted, ICP raises and this leads to a serious medical condition known as intracranial hypertension (IH). In a supine healthy adult, ICP can be up to 15 mmHg, whereas in critically ill patients the goal is to maintain ICP below 20 mmHg [1-2]. Sustained IH can be rapidly fatal and damage the brain [2]. Yet, IH is common in neurosurgical and neurological patients and thus, the monitoring of ICP and management of IH are both frequent and life-saving procedures. Causes of IH include intracranial mass lesions, disorders of CSF circulation, and more diffuse pathological processes [1–2].

In critical care setting, ICP is most commonly monitored from a catheter inserted into the ventricular system of the brain through a burr hole (ventriculostomy). This invasive method is considered a gold standard, because it is accurate and allows on-site recalibration as well as drainage of CSF to manage IH [1]. However, due to its invasiveness (patient discomfort) and risks of infection and hemorrhage [1–3] it is non-optimal for repeated and/or prolonged use beyond days. However, long-term ICP recording is highly desired in monitoring neurocritical care patients' recovery and in people who have an implanted cerebral shunt valve [4] to manage hydrocephalus [3][5].

On the other hand, the non-invasive methods are lack in accuracy and cannot be used for large number of patient due to anatomical variations [6]. To overcome the limitations of invasive and non-invasive methods, battery powered and fully passive implants have been reported in the recent literatures [7-11]. But these systems have their own limitations. The battery powered implants have large size and limited life time (due to battery life) whereas the fully passive implants have limited read range.

In contrast, we present a battery-free wirelessly powered implantable system for long-term monitoring of ICP. The proposed system overcomes the size and life-time limitations of a battery powered implant and read range limitation of a fully passive implant. The results presented in this article are continuation of our previous work [12-13]. In this paper, we present the pressure readout results in liquid after activating a piezoresistive pressure through inductive wireless powering.

II. SYSTEM DESIGN AND SIMULATION

Figure 1(a) presents the architecture of the proposed system. It consists of an implant and an external unit. The implant is powered wirelessly through inductively coupled antennas. The implant consists of a near field antenna for powering the implant, a piezoresistive pressure sensor, an energy harvesting unit and a data transmission unit. The external unit consists of a two-turn antenna and a matching circuitry. In the current work, the implant does not contain the data transmission unit, but the sensor output voltage was monitored through wires. The development of the data transmission unit is part of our ongoing work.

A. Antenna and wireless link modeling

We used ANSYS HFSS v15 in modeling of the inductive wireless link. As shown in Fig. 1(f), a 4-layer human head model is used and each tissue layer is assigned frequency dependent properties base on [14]. The external antenna is placed at a distance of 5 mm from the skin whereas the implant is placed beneath the scalp (see Fig. 1(f)). As explained in [15], the maximum of link power efficient for the coupled antennas is given by

$$G_{p,max} = \frac{\left|z_{21}\right|^2}{a + \sqrt{a^2 - \left|z_{12}z_{21}\right|^2}},\tag{2}$$
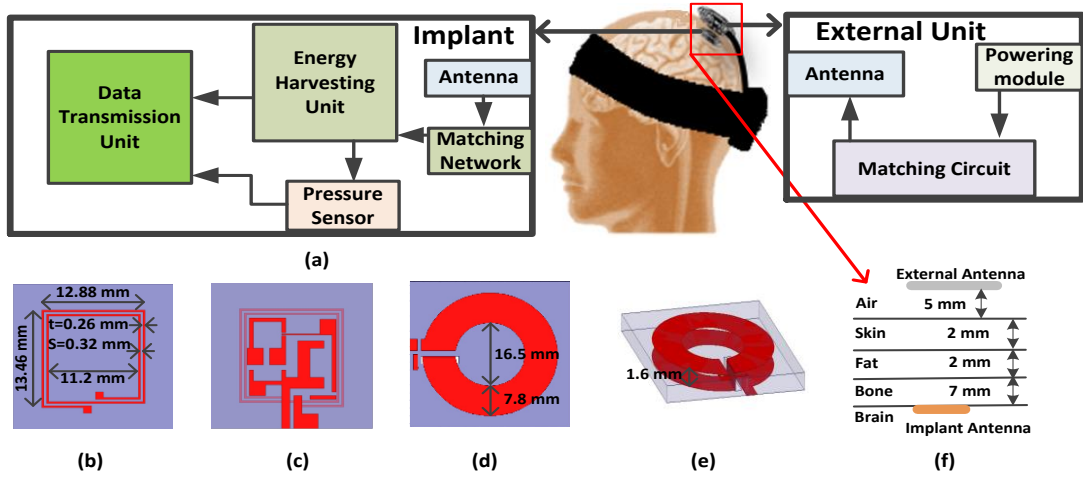
Fig. 1. (a) System level description of the implantable system (b) front side of implant antenna (c) back side of implant antenna for electronic components (d) top view of external antenna (e) side view of external antenna (f) human head layered simulation model of wireless link

where $a = 2\mathrm{Re}(z_{11})\mathrm{Re}(z_{22}) - \mathrm{Re}(z_{12}z_{21})$. The maximum allowed transmission power from an external antenna is limited by Specific Absorption Rate (SAR). We are following U.S. Federal Communications Commission (FCC) regulation (SAR_{max} = 1.6 W/kg). The maximum SAR-complaint transmission power, $P_{t,max}$ is computed based on SAR_{max} as explained in [15].

We used the same 2-turn loop antennas presented in [15] as an external antenna. As compared with a single-turn loop, it achieves lower SAR and same $G_{p,max}$ and thereby enables higher transmission power. The external antenna is implemented on FR4 substrate with the thickness of 1.6 mm. The external antenna inner loop diameter is 16.5 mm with trace width of 7.8 mm. Figs. 1(d) and (e) show the top and side views of the external antenna, respectively. The implant antenna consists of 2 coils and is implemented on a flexible polyimide substrate with the thickness of 50 μm, dielectric constant (ε_r) of 3.3 and tangent loss (tanδ) of 0.002. The implant dimensions are optimized for maximum link power efficiency as explained in [12]. Figs. 1(b) and (c) present the front and the back side of the implant.

Figure 2 shows the simulated $G_{p,max}$. The maximum of $G_{p,max}$ occurs at 5 MHz and starts to decline with increase in the frequency. The simulated maximum SAR-complaint transmission power ($P_{t,max}$) is presented in Fig. 3.

III. Measurement and Discussion

For the purpose of experimental characterization, an LC circuit was used to match the external antenna to 50 Ω system impedance. A capacitor in parallel sufficed for matching the implant antenna. However, due to very large component values and sensitivity of the matching networks toward variability in them, we are not able to resonate both antennas at the frequency of 5 MHz which was determined optimal in terms of link power efficiency in the simulations. Instead, we achieved matching at 11 MHz. As the simulated link power efficiency at 11 MHz was within 1 dB from the peak value (−3.63 dB) at 5 MHz, we conducted the experiments at 11 MHz. Fig. 4 shows the fabricated antennas and the measurement setup.
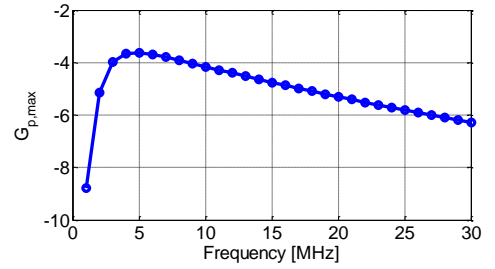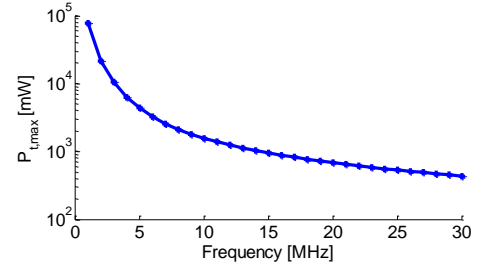

Fig. 2. Simulated link power efficiency ($G_{p,max}$)

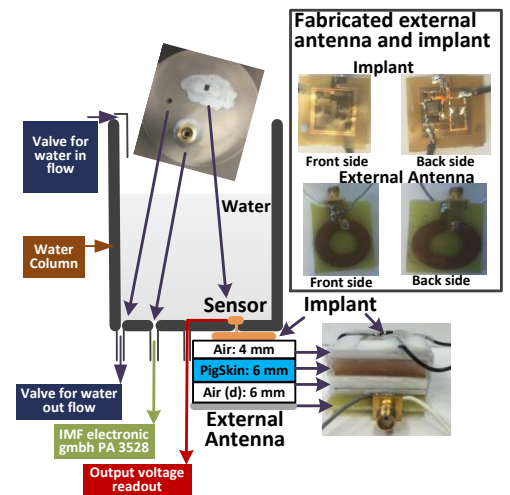Fig. 3. Simulated maximum SAR-compliant transmission power ($P_{t,max}$).

Fig. 4. Fabricated external antenna and implant, and the measurement setup.
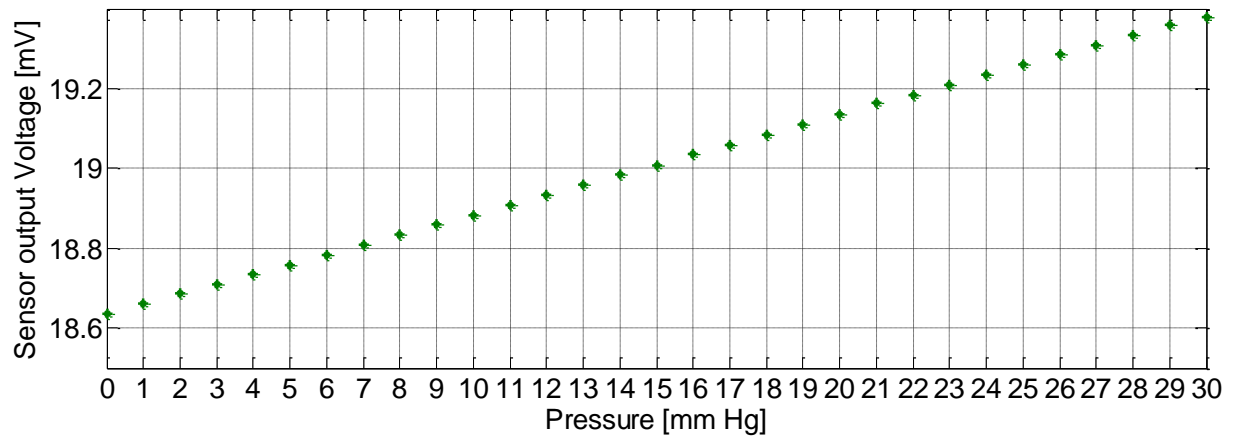
Fig. 5. Measured sensor output voltage with change in the pressure.

The antenna S-parameter were measured through Vector Network Analyzer (VNA). Port 1 is connected to the external antenna and port 2 to the implant antenna. The measured S-parameter are: S11 = –5.2 dB, S22= –9.42 dB and S21=S12= –15.77 dB. Two Schottky diodes (Skyworks SMS7630 series) in charge pump configuration along with a charge storage capacitor of 33 µF and a zener diode are used for RF-to-DC conversion. The piezoresistive sensor is connected after the zener diode.

We measured the sensor performance in liquid with change in the pressure. The pressure inside the water column is increased with the increase of water amount (see Fig. 4). There is 16 mm (10 mm air and 6 mm pig skin) distance between antennas and both antennas are centrally aligned. The pig skin is used to create the biological environment in-between the antennas. The sensor is coated with 2 µm Parylene C. After measurement setup, the external antenna is fed with a sine wave of 19.5 dBm. The measured voltage at sensor input terminals is 2.122 V, which remained constant throughout the measurement. After activating the sensor, the pressure inside the water column is increased with a step size of 1-mmHg. The output voltage of the sensor is measured against each pressure value. We used IMF electronics gmbh PA 3528 as a pressure reference device. Figure 5 shows the sensor output voltage with change in the pressure. The sensor shows linear response without any overlapping between the consecutive pressure readouts. Thus, it attests measurement accuracy with 1-mmHg resolution. Our ongoing work focuses on completion of the sensor data transmission unit.

REFERENCES

[1] L. A. Stainer, P. J. D. Adrews, "Monitoring the injured brain: ICP and CBF," British J. of Anesth., vol. 97, no. 1, pp. 26–38, May 2006.

[2] S. A. Mayer, Ji Y. Chong, "Critical care management of increased intracranial pressure," J. Intensive Care Med., vol. 17, no. 2, pp. 55–67, Mar. 2002.

[3] R. Beer, P. Lackner, B. Pfaust, E. Schutzhard, "Nosocomial ventriculitis and meningitis in neurocritical care patients," J. Neurol., vol. 255, no. 11, pp. 1617–1624, Nov. 2008.

[4] A. Aschoff, P. Kremer, B. Hashemi, S. Kunze, "The scientific history of hydrocephalus and its treatment," Neurosurg. Rev., vol. 22, pp. 67–93, Oct. 1999.

[5] F. B. Freimann, M. Schulz, H. Haberi, U.-W. Thomale, "Feasibility of telemetric ICP-guided valve adjustments for complex shunt therapy," Child's Nerv. Syst., vol. 30, no. 4, pp. 689–697, Apr. 2014.

[6] P. H. Raboel, J. Bartek Jr., M. Andresen, B. M. Bellander, B. Romner, "Intracranial pressure monitoring: invasive versus non-invasive methods – a review," Crit. Care Res. Pract., vol. 2012, article ID: 950393, Mar. 2012.

[7] U. Kawoos, M.-R. Tofighi, R. Warty, F. A. Kralick, A. Rosen, "In-vitro and in-vivo trans-scalp evaluation of an intracranial pressure implant at 2.4 GHz," IEEE Trans. Microw. Theory Techn., nol. 56, no. 10, pp. 2356–2365, Oct. 2008.

[8] K. Aquilina, M. Thoresen, E. Chakkarapani, I. K. Pople, H. B. Coakham, R. J. Edwards, "Preliminary evaluation of a novel intraparenchymal capacitive intracranial pressure monitor," J. Neurosurg., vol. 115, no. 3, pp. 561–569, May 2011.

[9] L. Y. Chen, B. C.-K. Tee, A. L. Chortos et al., "Continuous wireless pressure monitoring and mapping with ultra-small passive sensors for health monitoring and critical care," Nature Commun., vol. 5, article 5028, Oct. 2014.

[10] Mohammad H. Behfar, E. Moradi, T. Björninen, L. Sydänheimo, L. Ukkonen, "Biotelemetric wireless intracranial pressure monitoring: an in vitro study," Intl. J. Antennas Propag., vol. 2015, article ID 918698, Nov. 2015.

[11] S. Welschehold, E. Schmalhausen, P. Dodier, S. Vulcu, J. Oertel, W. Wagner, C. A. Tschan, "First clinical result with a new telemetric intracranial pressure-monitoring system," Neurosurg., vol. 70, pp. 44–49, Mar. 2012.

[12] M. W. A. Khan, T. Björninen, L. Sydänheimo, L. Ukkonen, "Remotely Powered Piezoresistive Pressure Sensor: Toward wireless monitoring of intracranial pressure," in IEEE Microwave and Wireless Components Letters , vol. 26, no. 7, pp.549-551, 2016.

[13] M. W. A. Khan, T. Björninen, M. Rizwan, L. Sydänheimo and L. Ukkonen, "Piezoresistive pressure sensor for ICP monitoring: remote powering through wearable textile antenna and sensor readout experiment," IEEE AP-S/URSI, Jun. 2016.

[14] S. Gabriel, R. W. Lau and C. Gabriel, "The dielectric properties of biological tissues: III. parametric models for the dielectric spectrum of tissues," Phys. Med. Biol., vol. 41, no. 11, pp. 2271–2293, Nov. 1996.

[15] M. W. A. Khan, T. Björninen, L. Sydänheimo and L. Ukkonen, "Characterization of Two-Turns External Loop Antenna with Magnetic Core for Efficient Wireless Powering of Cortical Implants," IEEE, Antennas Wireless Propag. Lett., vol. 15, pp. 1410-1413, Apr. 2016.